

Article

# Fully Automatic Operation Algorithm of Urban Rail Train Based on RBFNN Position Output Constrained Robust Adaptive Control

Junxia Yang \*, Youpeng Zhang \* and Yuxiang Jin

School of Electrical Engineering and Automation, Lanzhou Jiaotong University, Lanzhou 730070, China; zidonghuaxy@mail.lzjtu.cn

\* Correspondence: 0119046@stu.lzjtu.edu.cn (J.Y.); zhangyoupeng@mail.lzjtu.cn (Y.Z.)

**Abstract:** High parking accuracy, comfort and stability, and fast response speed are important indicators to measure the control performance of a fully automatic operation system. In this paper, aiming at the problem of low accuracy of the fully automatic operation control of urban rail trains, a radial basis function neural network position output-constrained robust adaptive control algorithm based on train operation curve tracking is proposed. Firstly, on the basis of the mechanism of motion mechanics, the nonlinear dynamic model of train motion is established. Then, RBFNN is used to adaptively approximate and compensate for the additional resistance and unknown interference of the train model, and the basic resistance parameter adaptive mechanism is introduced to enhance the anti-interference ability and adaptability of the control system. Lastly, on the basis of the RBFNN position output-constrained robust adaptive control technology, the train can track the desired operation curve, thereby achieving the smooth operation between stations and accurate stopping. The simulation results show that the position output-constrained robust adaptive control algorithm based on RBFNN has good robustness and adaptability. In the case of system parameter uncertainty and external disturbance, the control system can ensure high-precision control and improve the ride comfort.

**Keywords:** fully automatic operation system (FAO); radial basis function neural network (RBFNN); position output constrained control; adaptive control; tracking error



**Citation:** Yang, J.; Zhang, Y.; Jin, Y. Fully Automatic Operation Algorithm of Urban Rail Train Based on RBFNN Position Output Constrained Robust Adaptive Control. *Algorithms* **2021**, *14*, 264. <https://doi.org/10.3390/a14090264>

Academic Editor: Mircea-Bogdan Radac

Received: 15 August 2021  
Accepted: 7 September 2021  
Published: 9 September 2021

**Publisher's Note:** MDPI stays neutral with regard to jurisdictional claims in published maps and institutional affiliations.



**Copyright:** © 2021 by the authors. Licensee MDPI, Basel, Switzerland. This article is an open access article distributed under the terms and conditions of the Creative Commons Attribution (CC BY) license (<https://creativecommons.org/licenses/by/4.0/>).

## 1. Introduction

Urban rail transit's FAO (fully automatic operation system) is a direct control unit to ensure the safe operation of a train, and its advanced control algorithm is the core to ensure train control accuracy, comfort, and safe operation [1]. The use of an FAO controller with high control accuracy, less braking or traction switching times, and fast response speed is the key to ensure the safe and efficient operation of an urban rail train under a changeable operating environment and time-varying system status [2].

In the process of the development of the train FAO, FAO control algorithms have mainly included PID control [3], fuzzy control [4], neural network control [5], adaptive control [6], sliding mode control [7], predictive control [8], iterative learning [9], and the combination of various control methods [10]. The authors of [11] applied a train control algorithm based on fuzzy prediction to ensure the train's accurate tracking of the desired operation curve; however, the quadratic programming algorithm used in predictive control was time-consuming in the solution process, and the real-time performance was not easy to guarantee. The authors of [12] proposed an adaptive iterative learning control based on iterative variable parameters and measurement noise, which realized train operation control via the online modification of control parameters, but the real-time performance of continuous iteration was poor. The authors of [13] designed a sliding model using PID control for an automatic train operation system, which constrained the train operation

to the sliding hyperplane so as to realize tracking and accurate parking of the desired operation curve, but the influence of unknown disturbances on the train operation control was not considered, and the control accuracy could not be guaranteed under complex road conditions. The authors of [14] proposed an accurate parking control algorithm of an urban rail transit train based on adaptive terminal sliding mode control, which can adaptively adjust the control input according to the model parameter changes caused by the uncertainty of train dynamic model parameters and unknown disturbance to ensure that the train can accurately track the desired parking curve. However, too many control parameters were designed, which affected the response speed and control accuracy of the system. The authors of [15] proposed an automatic train operation speed control method based on active disturbance rejection control (ADRC). The unknown part of the train dynamics model was taken as the extended state to design a second-order ADRC. Although it had the advantages of strong anti-interference and small tracking error, the algorithm only considered the influence of basic resistance on the train operation when the train was operating on straight routes, whereas it did not consider the additional resistance caused by route conditions such as route curve and slope. However, the FAO control and optimization were typical nonlinear problems. On the one hand, the train operation is affected by many complex factors such as route conditions, external environment, unknown disturbances, and train performance. The complex and changeable train operation environment and the inevitable existence of modeling errors lead to the uncertainty and time-varying characteristics of system parameters, which increases the difficulty of control design. On the other hand, the strict requirements of simplicity and real-time operation of the FAO control algorithm ensure the engineering practicability of the designed algorithm. Therefore, in order to ensure the control performance indices of high-precision control, smooth operation, and fast response of the FAO, the above aspects must be fully considered in the design of FAO controller, so that the designed FAO control algorithm can be applied in engineering [16].

According to a review of a large number of FAO references, the existing control methods do not consider the complexity of the control or optimization algorithm structure, and they mostly use feedback to construct the control law, generating the control input through the deviation of the train operation status information. However, when the deviation of the train operating state from tracking the desired curve is large, the controller will generate a large fluctuating control input, which will affect the control accuracy of the train operation and the comfort of passengers. Therefore, this paper starts from a new perspective; based on the output-constrained adaptive control theory, while ensuring the minimum structural complexity of the algorithm, the upper and lower bounds of the output value of the train position are directly restricted, so as to ensure that the error of the train operation position is within the allowable error, the desired position curve is tracked with small position error or 0 error, and the control accuracy of the FAO is improved. Due to the influence of factors such as parameter uncertainty and external disturbance in the FAO, this paper introduces the additional resistance and unknown disturbances that cannot be accurately modeled in the train dynamics model into the position output-constrained adaptive controller in the form of disturbance by RBFNN, so as to enhance the ability of the system to deal with disturbances such as ramps and curves, as well as realize accurate tracking control of the urban rail train operation curve. This is of great significance for guaranteeing the safety of multi-train tracking operations and station fixed-point parking. The main elements of this paper are summarized below.

- A position output-constrained robust adaptive control algorithm based on RBFNN (RBFNN-POCRAC) is proposed. The algorithm combines position output constraints, RBFNN, and adaptive control, explicitly considers the complexity of the algorithm structure, the initial tracking, and approximation errors of the system, and gives the error boundary that can be adjusted to any small value by selecting appropriate parameters.

- Considering the unknown and time-varying coefficients of the basic resistance Davis equation, the adaptive control law is designed to estimate the basic resistance of the train and enhance the engineering practicability of the control algorithm.
- The additional resistance and unknown disturbance are introduced into the position output-constrained adaptive controller in the form of disturbance by RBFNN, which can usefully decrease the acquisition of data such as route slopes, curves, and turnouts, as well as have a strong inhibitory effect on the disturbance caused by train operation in open routes or tunnels.
- In order to test and verify the availability of the designed FAO controller, complex route conditions are selected for MATLAB simulation. The results show that the FAO control algorithm proposed in this paper can track the desired curve with higher control accuracy in a shorter time and has good control performance.

## 2. Train Dynamics Model

Considering the additional resistance and external disturbances in the process of train fully automatic operation, according to the principle of Newton dynamics, the time-based dynamic model of train single-particle motion can be described as follows:

$$\begin{cases} \dot{p}(t) = v(t) \\ m\dot{v}(t) = F(t) - g(v(t)) - f(p(t), v(t), t) \end{cases} \quad (1)$$

where  $m$  is the total mass of the whole train,  $p(t)$  is the train position,  $v(t)$  is the train speed,  $\dot{v}(t)$  is the train acceleration,  $F(t)$  is the train traction or brake force,  $g(v(t))$  is the basic resistance during train fully automatic operation, and  $f(p(t), v(t), t)$  is the additional resistance and other unknown disturbances that cannot be modeled.

The basic resistance refers to the resistance suffered by the train when running along the straight track, which is commonly described by the Davis Equation [17].

$$g(v(t)) = a_0 + b_0v(t) + c_0v^2(t), \quad (2)$$

where  $a_0$ ,  $b_0$ , and  $c_0$  are the basic resistance coefficients. The coefficients vary with different trains, operating environments, weather conditions, and other factors, leading to uncertainty in the parameters of the train dynamics model. Therefore, this paper introduces an adaptive control mechanism to cope with changes in train model parameters and ensure the control performance of the control system.

The additional resistance mainly refers to the route resistance affecting the train due to curves, ramps, or tunnels on the running route.

$$f(p(t), v(t), t) = \omega_r + \omega_i + \omega_s, \quad (3)$$

where  $\omega_r$ ,  $\omega_i$ , and  $\omega_s$  denote the additional resistance of the route curve, ramp, and tunnel.

Due to the effect of route curves, ramps, and tunnels, it is impossible to build an accurate model. In this paper, we consider the bounded time-varying dynamics and use RBFNN to approximate the unknown nonlinear additional resistance and unknown disturbance function.

Define  $x_1 = p(t)$ ,  $x_2 = v(t)$ ; thus, Equation (1) is rewritten as follows:

$$\begin{cases} \dot{x}_1 = x_2 \\ \dot{x}_2 = u + g + f(x) \end{cases} \quad (4)$$

where  $x_1 = p(t)$  and  $x_2 = v(t)$  are the train position and train speed,  $u = \frac{F(t)}{m}$  is the control input of the FAO controller,  $g = -\frac{g(x_2)}{m}$  is the basic resistance, and  $f(x) = -\frac{f(x_1, x_2, t)}{m}$  is the additional resistance and other unknown disturbances that cannot be modeled.

**Assumption 1.** *The dynamics system of train operation given in Equation (4) is an input-state stable system.*

### 3. Resistance Analysis Based on RBFNN

When the train operates under the actual route conditions with large slopes and small curves, the additional resistance and unknown disturbances caused by the complex route may be large, leading to a low accuracy of train control and affecting the safety of train operation. Therefore, RBFNN is used to learn and estimate the additional resistance and unknown disturbance in the train dynamics model, which mainly solves the problem of the large position and speed tracking error caused by factors such as dynamic model simplification, model parameter uncertainty, and external environment change in order to enhance the adaptability and anti-interference performance of the FAO.

RBFNN is a locally convergent forward network, which has simple structure, fast learning speed, and good generalization ability. Theoretically, it can approximate any smooth function with any precision, which can be regarded as a universal approximator [18,19]. There are many research results in the adaptive control of nonlinear systems [20–22].

The structure of RBFNN is shown in Figure 1, which is composed of three layers of a forward network. The input layer is composed of signal source nodes. The number of neurons in the hidden layer depends on the exact requirements of the approximation function. The output layer outputs the response to the input layer. The mapping from input to output is nonlinear, while the mapping from hidden layer to output space is linear, which speeds up learning and effectively avoids the local minimum problem [23–26]. The output of the output layer is the linear weighted sum of the output signals of the hidden layer, and the ‘weight’ represents the adjustable parameters of the network structure. By adjusting the appropriate output weight, the RBFNN can realize the approximation of the unknown nonlinear additional resistance and disturbance function.

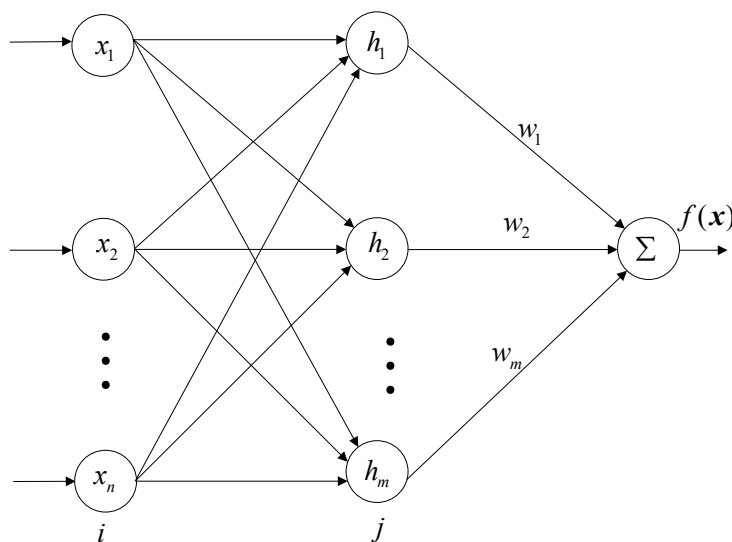


Figure 1. Structure of RBFNN.

In Figure 1,  $\mathbf{x} = [x_1, x_2, \dots, x_n]^T \in R^n$  is the network input,  $n$  is the dimension of the input vector,  $\mathbf{W} = [w_1, w_2, \dots, w_m]^T$  is an adjustable weight parameter vector,  $m$  is the number of neurons in the hidden layer,  $\mathbf{h}(\mathbf{x}) = [h_1(\mathbf{x}), h_2(\mathbf{x}), \dots, h_m(\mathbf{x})]^T$  is the output vector of Gaussian function for the hidden layer, and  $h_j(\mathbf{x})$  is the output of the  $j$ -th neuron in the hidden layer.  $h_j(\mathbf{x})$  can be expressed as follows:

$$h_j(\mathbf{x}) = \exp\left(-\frac{\|\mathbf{x} - c_j\|^2}{2b_j^2}\right) \quad j = 1, 2, \dots, m, \tag{5}$$

where  $\|\cdot\|$  is a Euclidean norm, and  $c_j$  and  $b_j$  are the center parameter and width parameter of the Gaussian function of the  $j$ -th neuron in the hidden layer. The width vector of the

hidden layer Gaussian function is  $\mathbf{b} = [b_1, b_2, \dots, b_m]^T$ , and  $b_j > 0$ . The coordinate vector of the center point of the hidden layer Gaussian function is as follows:

$$\mathbf{c} = [c_{j1}, c_{j2}, \dots, c_{ji}, \dots, c_{jn}]^T \quad i = 1, 2, \dots, n. \tag{6}$$

RBFNN can approximate the unknown nonlinear additional resistance and interference function with any precision in the compact working domain  $\Theta_x \subset R^n$ .  $f(\mathbf{x})$  is as follows:

$$f(\mathbf{x}) = \mathbf{W}^{*T} \mathbf{h}(\mathbf{x}) + \varepsilon(\mathbf{x}), \tag{7}$$

where  $\mathbf{W}^*$  is the weight vector that minimizes  $\varepsilon(\mathbf{x})$  among all the estimated weights, in which

$$\mathbf{W}^* = \arg \min_{\mathbf{W} \in R^m} \left\{ \sup_{\mathbf{x} \in \Theta_x} |f(\mathbf{x}) - \mathbf{W}^T \mathbf{h}(\mathbf{x})| \right\}, \tag{8}$$

where  $\varepsilon(\mathbf{x})$  is a bounded approximation error; that is, there is a small normal  $\varepsilon^*$  number satisfying  $|\varepsilon(\mathbf{x})| \leq \varepsilon^*$ .

The performance index of the RBFNN output layer is as follows:

$$E = 0.5 [f(\mathbf{x}) - \hat{f}(\mathbf{x})]^2, \tag{9}$$

where  $\hat{f}(\mathbf{x})$  is the RBFNN output.

In the RBFNN structure, appropriate selection of the hidden layer node center, basis function width, and weight parameters can enhance convergence speed and approximation accuracy. According to the gradient descent method, the iterative algorithms of output weight, node center, and node basis function width parameters are as follows:

$$\Delta w_j(t) = \eta [f(\mathbf{x}) - \hat{f}(\mathbf{x})] h_j, \tag{10}$$

$$w_j(t) = w_j(t-1) + \Delta w_j(t) + \varpi [w_j(t-1) - w_j(t-2)], \tag{11}$$

$$\Delta b_j = \eta [f(\mathbf{x}) - \hat{f}(\mathbf{x})] w_j h_j \frac{\|\mathbf{x} - \mathbf{c}_j\|^2}{b_j^3}, \tag{12}$$

$$b_j(t) = b_j(t-1) + \Delta b_j + \varpi [b_j(t-1) - b_j(t-2)], \tag{13}$$

$$\Delta c_{ji} = \eta [f(\mathbf{x}) - \hat{f}(\mathbf{x})] w_j h_j \frac{x_i - c_{ji}^2}{b_j^2}, \tag{14}$$

$$c_{ji}(t) = c_{ji}(t-1) + \Delta c_{ji} + \varpi [c_{ji}(t-1) - c_{ji}(t-2)], \tag{15}$$

where  $\eta \in (0, 1)$  is the learning rate, and  $\varpi \in (0, 1)$  is the momentum factor.

The RBFNN input is  $\mathbf{x} = [x_1 \quad x_2]^T$ , and the output is as follows:

$$\hat{f}(\mathbf{x}) = \hat{\mathbf{W}}^T \mathbf{h}(\mathbf{x}) \tag{16}$$

The error function is defined as

$$\tilde{f}(\mathbf{x}) = f(\mathbf{x}) - \hat{f}(\mathbf{x}) = \mathbf{W}^{*T} \mathbf{h}(\mathbf{x}) + \varepsilon(\mathbf{x}) - \hat{\mathbf{W}}^T \mathbf{h}(\mathbf{x}) = -\tilde{\mathbf{W}}^T \mathbf{h}(\mathbf{x}) + \varepsilon(\mathbf{x}), \tag{17}$$

where  $\tilde{\mathbf{W}} = \hat{\mathbf{W}} - \mathbf{W}^*$  is the estimation error of the weight vector.

**Assumption 2.**  $f(\mathbf{x})$  is time-varying and bounded; that is, there is an unknown constant  $f^*$ , which satisfies  $|f(\mathbf{x})| \leq f^*$ .

#### 4. Design of Position Output-Constrained Robust Adaptive Control

The control problem of a constrained system is one of the most studied fields in control theory and engineering application [27]. In FAO, in order to ensure the safety of multiple train tracking operation and station fixed-point parking, it is necessary to make strict restrictions on the upper and lower bounds of the train position output value. The theoretical basis for designing the position output-constrained robust adaptive controller is as follows:

**Lemma 1** ([28]). Consider the following error system:

$$\dot{e} = f(t, e), \tag{18}$$

where  $e = [e_1 \ e_2]^T$ ,  $e_1$  and  $e_2$  are the position error and speed error.

These are functions with continuous differentiable and positive definite  $V_1$  and  $V_2$ ,  $k > 0$ , where  $x_1$  is position output, and  $x_d$  is desired position output. The position error  $e_1 = x_1 - x_d$  is defined, when the following conditions are satisfied:

1. When  $e_1 \rightarrow -k$  or  $e_1 \rightarrow k$ ,  $V_1(e_1) \rightarrow \infty$ ;
2.  $\chi_1(\|e_2\|) \leq V_2(e_2) \leq \chi_2(\|e_2\|)$ , where  $\chi_1$  and  $\chi_2$  are  $K_\infty$  class functions.

It is assumed that  $|e_1(0)| < k$ , taking  $V(e) = V_1(e_1) + V_2(e_2)$ , if  $V(e)$  can satisfy

$$\dot{V} = \frac{\partial V}{\partial x} f \leq -\mu V + l, \tag{19}$$

where  $l > 0$  and is bounded.

Thus,  $|e_1(t)| < k, \forall t \in [0, \infty)$ .

Consider the following symmetric Barrier Lyapunov function [29]:

$$V_1(e_1) = \frac{1}{2} \log \frac{k^2}{k^2 - e_1^2}, \tag{20}$$

where  $\log(\cdot)$  is natural logarithm.

It can be seen that the Lyapunov function satisfies the  $V(0) = 0, V(x) > 0 (x \neq 0)$  Lyapunov design principle.

It can be seen from  $\dot{V} \leq -\mu V + \lambda$  that  $V$  is a bounded. Due to  $V$  being a continuous function,  $V_1 = \frac{1}{2} \log \frac{k^2}{k^2 - e_1^2}$ . The initial state satisfies  $|e_1(0)| < k$ , and  $e_1^2 \neq k^2$ ; that is,  $\forall t \in [0, \infty), |e_1(t)| < k$ .

In this paper, the maximum position error is constrained as  $e_1(t) = 0.2$ , due to  $|e_1(t)| < k$ ; taking  $k = 0.21$ , the input and output results of the symmetric Barrier Lyapunov function are shown in Figure 2.

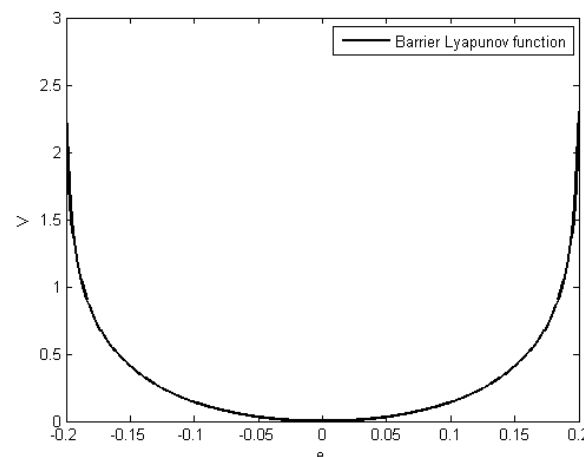


**Figure 2.** Symmetric barrier Lyapunov function.

**Lemma 2** ([28]). For  $k > 0$ , if  $|e_1(t)| < k, \forall t \in [0, \infty)$ , then

$$\log \frac{k^2}{k^2 - e_1^2} < \frac{e_1^2}{k^2 - e_1^2}. \quad (21)$$

## 5. RBFNN Design and Analysis of Position Output-Constrained Robust Adaptive Controller

The objectives of the FAO controller design are as follows:

- When the coefficients of the basic resistance Davis equation are uncertain or time-varying, the additional resistance cannot be accurately modeled, and the disturbance is unknown, the train can track the desired speed and position curve with high precision, ensuring that the tracking error during train operation converges to a sufficiently small area quantified by the control parameter.
- The FAO is stable; that is, all closed-loop signals are bounded.

### 5.1. Control Algorithm Design

In order to achieve the above control objectives, on the basis of the backstepping method and Lyapunov integration analysis and design, the adaptive control law and parameter learning update law were designed to ensure the adaptability and robustness of the designed controller.

The position tracking error and its derivative signal are defined as follows:

$$e_1 = x_1 - x_d, \quad (22)$$

$$e_2 = x_2 - r, \quad (23)$$

where  $r$  is the virtual control law to be designed, and  $x_d$  is the known train position information, i.e., the desired position.

**Assumption 3.** The desired position  $x_d$  and its first-order derivatives  $\dot{x}_d$  and second-order derivatives  $\ddot{x}_d$  are known and bounded.

The two-side differential of  $e_1$  is obtained as follows:

$$\dot{e}_1 = \dot{x}_1 - \dot{x}_d = x_2 - \dot{x}_d. \quad (24)$$

The two-side differential of  $\dot{e}_2$  is obtained as follows:

$$\begin{aligned} \dot{e}_2 &= \dot{x}_2 - \dot{r} \\ &= u + g + f(\mathbf{x}) - \dot{r} \\ &= u - \frac{a_0}{m} - \frac{b_0}{m}x_2 - \frac{c_0}{m}x_2^2 + f(\mathbf{x}) - \dot{r}. \end{aligned} \quad (25)$$

By differentiating the two sides of the symmetric Barrier Lyapunov function  $V_1$  of Equation (20), it can be obtained that

$$\dot{V}_1 = \frac{e_1 \dot{e}_1}{k^2 - e_1^2} = \frac{e_1(x_2 - \dot{x}_d)}{k^2 - e_1^2} = \frac{e_1(e_2 + r - \dot{x}_d)}{k^2 - e_1^2}. \quad (26)$$

The design virtual control law is expressed as

$$r = -\alpha e_1 + \dot{x}_d, \quad (27)$$

where  $\alpha > 0$  represents the control parameters to be designed.

The two-side differential of  $r$  is obtained as follows:

$$\dot{r} = -\alpha \dot{e}_1 + \ddot{x}_d. \quad (28)$$

By substituting Equation (27) into Equation (26), we can get

$$\dot{V}_1 = -\frac{\alpha e_1^2}{k^2 - e_1^2} + \frac{e_1 e_2}{k^2 - e_1^2}. \tag{29}$$

The Lyapunov function is defined as

$$V_2 = V_1 + \frac{1}{2}e_2^2. \tag{30}$$

The two-side differential of  $V_2$  is obtained as follows:

$$\dot{V}_2 = \dot{V}_1 + e_2 \dot{e}_2 = -\frac{\alpha e_1^2}{k^2 - e_1^2} + \frac{e_1 e_2}{k^2 - e_1^2} + e_2 \dot{e}_2. \tag{31}$$

By substituting Equation (25) into Equation (31), we can get

$$\dot{V}_2 = -\frac{\alpha e_1^2}{k^2 - e_1^2} + \frac{e_1 e_2}{k^2 - e_1^2} + e_2[u - \frac{a_0}{m} - \frac{b_0}{m}x_2 - \frac{c_0}{m}x_2^2 + f(x) - \dot{r}]. \tag{32}$$

**Assumption 4.** The control input  $u$  is time-varying and bounded; that is, there is an unknown constant  $u^*$  satisfying  $|u| \leq u^*$ .

The control law and adaptive law are designed as follows:

$$u = \hat{a} + \hat{b}x_2 + \hat{c}x_2^2 - \hat{f}(x) + \dot{r} - \beta e_2 - \frac{e_1}{k^2 - e_1^2}, \tag{33}$$

$$\dot{\hat{a}} = -\lambda_1(e_2 + \sigma_1 \hat{a}), \tag{34}$$

$$\dot{\hat{b}} = -\lambda_2(x_2 e_2 + \sigma_2 \hat{b}), \tag{35}$$

$$\dot{\hat{c}} = -\lambda_3(x_2^2 e_2 + \sigma_3 \hat{c}), \tag{36}$$

$$\dot{\hat{W}} = \chi e_2 h(x) - \chi \hat{W}, \tag{37}$$

where  $\hat{a}$ ,  $\hat{b}$ , and  $\hat{c}$  are the estimated values of  $\frac{a_0}{m} = a^*$ ,  $\frac{b_0}{m} = b^*$ , and  $\frac{c_0}{m} = c^*$ , respectively,  $\tilde{a} = \hat{a} - a^*$ ,  $\tilde{b} = \hat{b} - b^*$ , and  $\tilde{c} = \hat{c} - c^*$  are the estimated error values,  $\beta > 0$  and  $\chi > 0$  are design parameters,  $\hat{f}(x)$  is the estimated value of  $f(x)$ , and  $\lambda_i$  and  $\sigma_i$ ,  $i = 1, 2, 3$  are adaptive parameters.

**Assumption 5.** The parameters satisfy  $|a^*| \leq a^\dagger$ ,  $|b^*| \leq b^\dagger$ , and  $|c^*| \leq c^\dagger$ , where  $a^\dagger$ ,  $b^\dagger$ , and  $c^\dagger$  are unknown and bounded values.

### 5.2. System Stability Analysis

**Theorem 1.** According to the train dynamics model in Equation (4), under all assumptions, based on RBFNN, adaptive and position output-constrained control theory, the adaptive control laws in Equations (27) and (33), adaptive laws of the basic resistance coefficients in Equations (34)–(36), and adaptive law of weight vector in RBFNN approximating additional resistance and unknown disturbance in Equation (37) are designed. Then, the train can track the given train operating curve with high precision in real time under the condition of the uncertain basic resistance coefficient, additional resistance, and unknown disturbance, and the tracking error will converge to a small enough neighborhood quantified by the designed control parameter, whereby the FAO is stable. The initial state of the closed-loop FAO system is as follows:

$$\frac{1}{2} \log \frac{k^2}{k^2 - e_1^2(0)} + \frac{1}{2} e_2^2(0) + \frac{1}{2\chi} \tilde{W}^2(0) + \frac{1}{2\lambda_1} \tilde{a}^2(0) + \frac{1}{2\lambda_2} \tilde{b}^2(0) + \frac{1}{2\lambda_3} \tilde{c}^2(0) \leq \zeta,$$

where,  $\zeta$  is any positive constant, and  $\alpha, \beta, \chi, \lambda_i, \sigma_i$ , and  $i = 1, 2, 3$  are control parameters.

**Proof of Theorem 1.** The Lyapunov function is chosen as follows:

$$V = \frac{1}{2} \log \frac{k^2}{k^2 - e_1^2} + \frac{1}{2} e_2^2 + \frac{1}{2\chi} \tilde{W}^T \tilde{W} + \frac{1}{2\lambda_1} \tilde{a}^2 + \frac{1}{2\lambda_2} \tilde{b}^2 + \frac{1}{2\lambda_3} \tilde{c}^2. \tag{38}$$

The two-side differential of  $V$  is obtained as follows:

$$\dot{V} = -\frac{\alpha e_1^2}{k^2 - e_1^2} + \frac{e_1 e_2}{k^2 - e_1^2} + e_2 \dot{e}_2 + \frac{1}{\chi} \tilde{W}^T \dot{\tilde{W}} + \frac{1}{\lambda_1} \tilde{a} \dot{\tilde{a}} + \frac{1}{\lambda_2} \tilde{b} \dot{\tilde{b}} + \frac{1}{\lambda_3} \tilde{c} \dot{\tilde{c}}. \tag{39}$$

By substituting the control law of Equation (33) into Equation (25), we can get

$$\begin{aligned} \dot{e}_2 &= \hat{a} + \hat{b}x_2 + \hat{c}x_2^2 - \hat{f}(x) + \dot{r} - \beta e_2 - \frac{e_1}{k^2 - e_1^2} - a^* - b^*x_2 - c^*x_2^2 + f(x) - \dot{r} \\ &= \tilde{a} + \tilde{b}x_2 + \tilde{c}x_2^2 + \tilde{f}(x) - \beta e_2 - \frac{e_1}{k^2 - e_1^2} \\ &= \tilde{a} + \tilde{b}x_2 + \tilde{c}x_2^2 - \beta e_2 - \frac{e_1}{k^2 - e_1^2} - \tilde{W}^T h(x) + \varepsilon(x) \end{aligned} \tag{40}$$

By substituting Equation (40) and the designed adaptive laws of Equations (34)–(37) into Equation (39), we can get

$$\begin{aligned} \dot{V} &= -\frac{\alpha e_1^2}{k^2 - e_1^2} + \frac{e_1 e_2}{k^2 - e_1^2} + e_2 \left[ \tilde{a} + \tilde{b}x_2 + \tilde{c}x_2^2 - \beta e_2 - \frac{e_1}{k^2 - e_1^2} - \tilde{W}^T h(x) + \varepsilon(x) \right] \\ &\quad + \frac{1}{\chi} \tilde{W}^T [\chi e_2 h(x) - \chi \dot{\tilde{W}}] + \frac{1}{\lambda_1} \tilde{a} [-\lambda_1 (e_2 + \sigma_1 \hat{a})] \\ &\quad + \frac{1}{\lambda_2} \tilde{b} [-\lambda_2 (x_2 e_2 + \sigma_2 \hat{b})] + \frac{1}{\lambda_3} \tilde{c} [-\lambda_3 (x_2^2 e_2 + \sigma_3 \hat{c})] \\ &= -\frac{\alpha e_1^2}{k^2 - e_1^2} + \frac{e_1 e_2}{k^2 - e_1^2} + e_2 \left[ \tilde{a} + \tilde{b}x_2 + \tilde{c}x_2^2 - \beta e_2 - \frac{e_1}{k^2 - e_1^2} - \tilde{W}^T h(x) + \varepsilon(x) \right] \\ &\quad + e_2 \tilde{W}^T h(x) - \tilde{W}^T \dot{\tilde{W}} - \tilde{a} e_2 - \sigma_1 \tilde{a} \hat{a} - \tilde{b} x_2 e_2 - \sigma_2 \tilde{b} \hat{b} - \tilde{c} x_2^2 e_2 - \sigma_3 \tilde{c} \hat{c} \\ &= -\frac{\alpha e_1^2}{k^2 - e_1^2} - \beta e_2^2 + e_2 \varepsilon(x) - \tilde{W}^T \dot{\tilde{W}} - \sigma_1 \tilde{a} \hat{a} - \sigma_2 \tilde{b} \hat{b} - \sigma_3 \tilde{c} \hat{c} \end{aligned} \tag{41}$$

According to Lemma 2, we know that

$$-\frac{\alpha e_1^2}{k^2 - e_1^2} < -\alpha \log \frac{k^2}{k^2 - e_1^2}. \tag{42}$$

According to Young’s inequality properties, we can get

$$e_2 \varepsilon(x) \leq \frac{1}{2} e_2^2 + \frac{1}{2} \varepsilon^{*2}, \tag{43}$$

$$-\tilde{W}^T \dot{\tilde{W}} = -\tilde{W}^T (\tilde{W} + W^*) = -\tilde{W}^T \tilde{W} - \tilde{W}^T W^* \leq -\frac{1}{2} \tilde{W}^T \tilde{W} + \frac{1}{2} W^{*2}, \tag{44}$$

$$-\sigma_1 \tilde{a} \hat{a} \leq -\frac{1}{2} \sigma_1 \tilde{a}^2 + \frac{1}{2} \sigma_1 a^{*2}, \tag{45}$$

$$-\sigma_2 \tilde{b} \hat{b} \leq -\frac{1}{2} \sigma_2 \tilde{b}^2 + \frac{1}{2} \sigma_2 b^{*2}, \tag{46}$$

$$-\sigma_3 \tilde{c} \hat{c} \leq -\frac{1}{2} \sigma_3 \tilde{c}^2 + \frac{1}{2} \sigma_3 c^{*2}. \tag{47}$$

By substituting Equations (42)–(47) into Equation (41), we can get

$$\begin{aligned} \dot{V} \leq & -\alpha \log \frac{k^2}{k^2 - e_1^2} - (\beta - \frac{1}{2})e_2^2 - \frac{1}{2}\tilde{\mathbf{W}}^T \tilde{\mathbf{W}} - \frac{1}{2}\sigma_1 \tilde{a}^2 - \frac{1}{2}\sigma_2 \tilde{b}^2 - \frac{1}{2}\sigma_3 \tilde{c}^2 \\ & + \frac{1}{2}\varepsilon^{*2} + \frac{1}{2}\mathbf{W}^{*2} + \frac{1}{2}\sigma_1 a^{*2} + \frac{1}{2}\sigma_2 b^{*2} + \frac{1}{2}\sigma_3 c^{*2} \end{aligned} \tag{48}$$

Accordingly, the following can be defined:

$$\mu = \min[2\alpha, 2\beta - 1, \chi, \lambda_1\sigma_1, \lambda_2\sigma_2, \lambda_3\sigma_3], \tag{49}$$

$$l = \frac{1}{2}\varepsilon^{*2} + \frac{1}{2}\mathbf{W}^{*2} + \frac{1}{2}\sigma_1 a^{*2} + \frac{1}{2}\sigma_2 b^{*2} + \frac{1}{2}\sigma_3 c^{*2}. \tag{50}$$

Thus,

$$\begin{aligned} \dot{V} \leq & -\mu \left[ \frac{1}{2} \log \frac{k^2}{k^2 - e_1^2} + \frac{1}{2}e_2^2 + \frac{1}{2\chi} \tilde{\mathbf{W}}^T \tilde{\mathbf{W}} + \frac{1}{2\lambda_1} \tilde{a}^2 + \frac{1}{2\lambda_2} \tilde{b}^2 + \frac{1}{2\lambda_3} \tilde{c}^2 \right] + l \\ \leq & -\mu V + l \end{aligned} \tag{51}$$

By selecting the appropriate control parameters  $\alpha, \beta, \chi, \lambda_i$  and  $\sigma_i, \mu > \frac{1}{\zeta}$  can be satisfied. If  $V > \zeta$ , then  $\dot{V} < 0$ ; that is,  $V \leq \zeta$  is an invariant set. If  $V(0) \leq \zeta$  holds, then  $\forall t \geq 0$ ; that is,  $V(t) \leq \zeta$ .

According to Lemma 1, we can know that  $V$  is bounded, and  $|e_1| < k$ . Accordingly, all error signals  $e_1, e_2, \tilde{\mathbf{W}}, \tilde{a}, \tilde{b}$ , and  $\tilde{c}$  are bounded; thus,  $\hat{\mathbf{W}}, \hat{a}, \hat{b}$ , and  $\hat{c}$  are bounded. According to Equation (51), it can be concluded that

$$0 \leq V(t) \leq \frac{l}{\mu} + [V(0) - \frac{l}{\mu}] \exp^{-\mu t}. \tag{52}$$

The inequality in Equation (52) means that there is a moment  $T$ , and, for  $\forall t > T, 0 \leq V(t) \leq \frac{l}{\mu}$  is always established. According to Equation (38), we can get that  $e_2, \tilde{\mathbf{W}}, \tilde{a}, \tilde{b}$ , and  $\tilde{c}$  converge to the following compact sets, respectively:

$$\Omega_{e_2} = \left\{ e_2 \mid |e_2| \leq \sqrt{\frac{2l}{\mu}} \right\}, \tag{53}$$

$$\Omega_{\tilde{\mathbf{W}}} = \left\{ \tilde{\mathbf{W}} \mid |\tilde{\mathbf{W}}| \leq \sqrt{\frac{2\chi l}{\mu}} \right\}, \tag{54}$$

$$\Omega_{\tilde{a}} = \left\{ \tilde{a} \mid |\tilde{a}| \leq \sqrt{\frac{2\lambda_1 l}{\mu}} \right\}, \tag{55}$$

$$\Omega_{\tilde{b}} = \left\{ \tilde{b} \mid |\tilde{b}| \leq \sqrt{\frac{2\lambda_2 l}{\mu}} \right\}, \tag{56}$$

$$\Omega_{\tilde{c}} = \left\{ \tilde{c} \mid |\tilde{c}| \leq \sqrt{\frac{2\lambda_3 l}{\mu}} \right\}. \tag{57}$$

From the above content, it can be seen that the tracking error of the FAO can be adjusted to any small value by selecting the appropriate control parameters. In addition, the initial estimation errors  $\tilde{\mathbf{W}}(0), \tilde{a}(0), \tilde{b}(0)$ , and  $\tilde{c}(0)$ , and their influence on the system performance can also be adjusted to any small value by selecting appropriate control parameters. □

### 6. Simulation Experimental Results

In this paper, MATLAB 2018a simulations were divided into two parts. The first used the actual parameters of urban rail trains to carry out the RBFNN position output-constrained robust adaptive control (RBFNN-POCRAC) design and desired curve tracking. Then, with the same train parameters and desired curve, the position output-constrained robust adaptive control (POCRAC) without RBFNN approximation of additional resistance and unknown disturbance, using the PID controller and the RBFNN-PID controller in the literature [30], was selected for performance comparison. The desired speed and position curve of the train tracking target is shown in Figure 3. The parameter information of the train route such as the slope and curve radius is shown in Table 1. Equation (4) was selected as the train dynamics model. The basic resistance simulation parameters were set as  $a^* = 0.3, b^* = 4 \times 10^{-3}, c^* = 1.6 \times 10^{-4}$ .

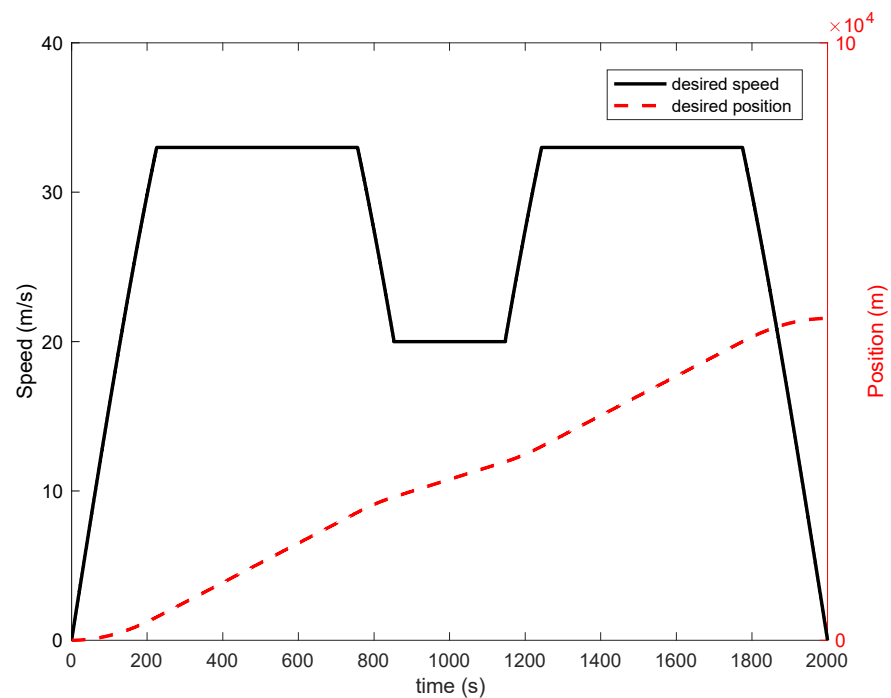


Figure 3. Desired speed and position profiles of train operation.

Table 1. Parameters for route condition.

Parameters	Range	Value
Slope/(‰)	0–3800	2
	3800–9200	−1.5
	9200–21,400	0
	21,400–23,900	5
	23,900–29,900	2.5
	29,900–32,300	−3
	32,300–50,000	0
	50,000–53,880	1.2
Curve (m)	0–4600	1000
	4600–18,000	1200
	18,000–24,200	800
	24,200–29,300	1500
	29,300–34,000	700
	34,000–48,000	1300
	48,000–53,880	1200

The additional resistance caused by the route condition.

6.1. Simulation of RBFNN Position Output-Constrained Robust Adaptive Controller

In the simulation environment of Theorem 1, the input variable of RBFNN was  $x = [x_1 \ x_2]^T$ ,  $\eta = 0.2$ ,  $\omega = 0.04$ . The control parameters were set as  $\alpha = 0.5$ ,  $\beta = 0.51$ ,  $\lambda_1 = 0.01$ ,  $\lambda_2 = 0.01$ ,  $\lambda_3 = 0.01$ ,  $\sigma_1 = 0.005$ ,  $\sigma_2 = 0.005$ ,  $\sigma_3 = 0.005$ ,  $\chi = 0.1$ ,  $k = 0.21$ . The initial state was selected as  $x_1(0) = 0$ ,  $x_2(0) = 0$ . The initial parameters were  $\hat{a} = 0.25$ ,  $\hat{b} = 0$ , and  $\hat{c} = 0$ . For the desired speed and position curve given in Figure 3, the tracking simulation results of the RBFNN-POCRAC controller are shown in Figures 4–8.

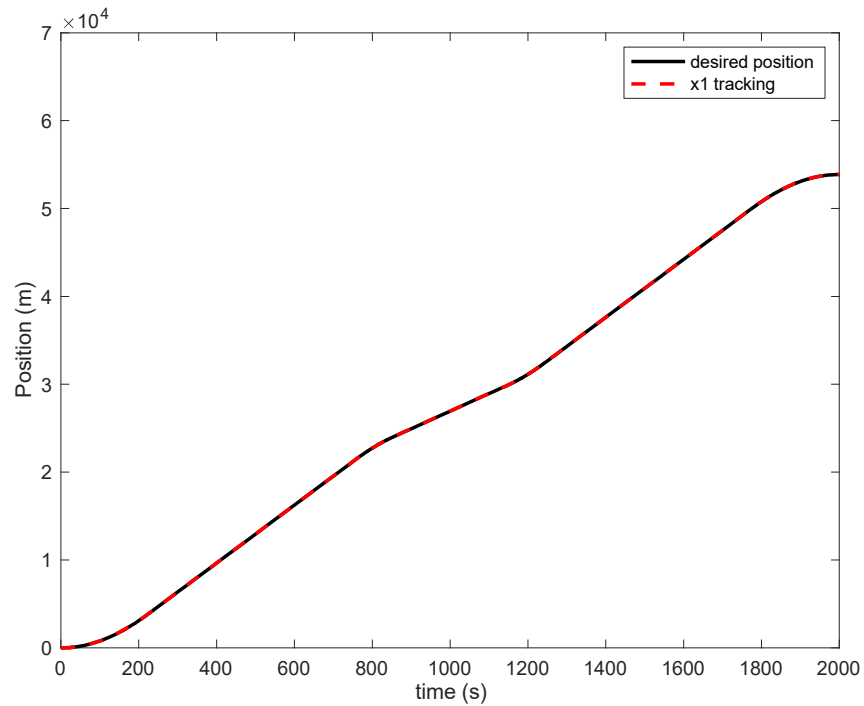


Figure 4. Position tracking performance.

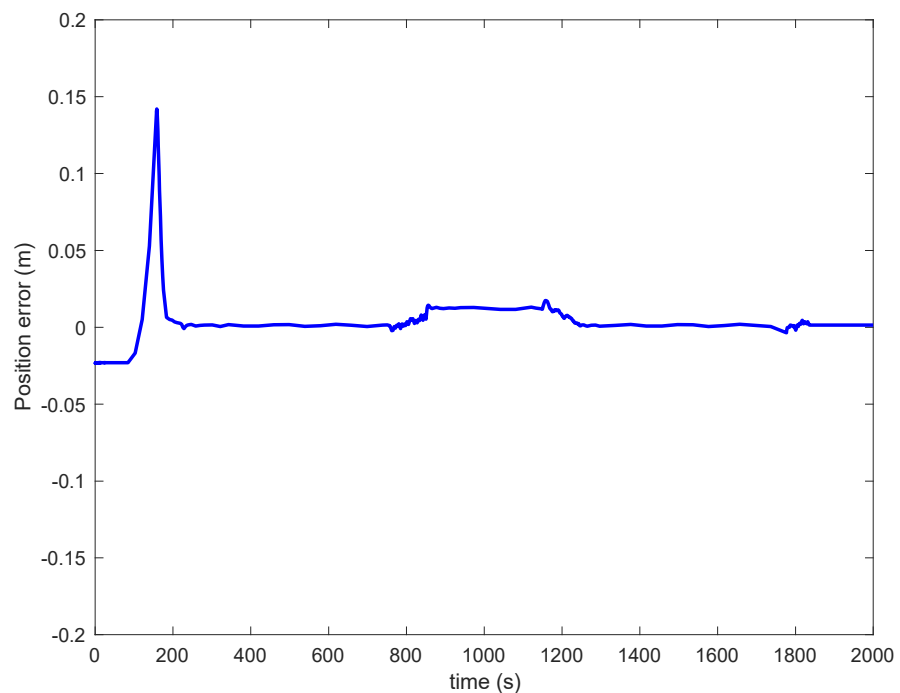


Figure 5. Position error.

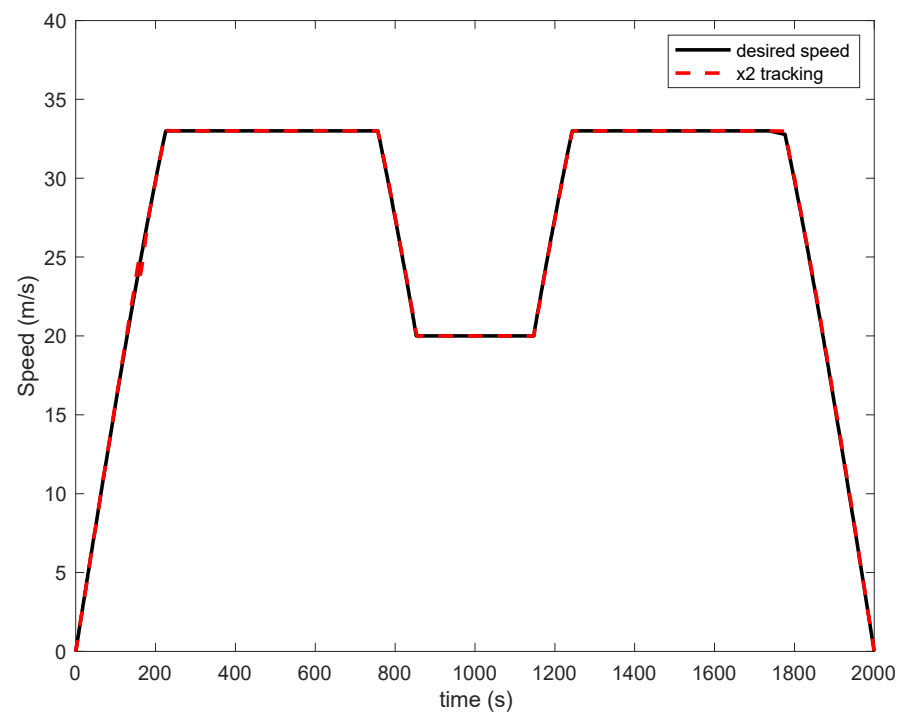


Figure 6. Speed tracking performance.

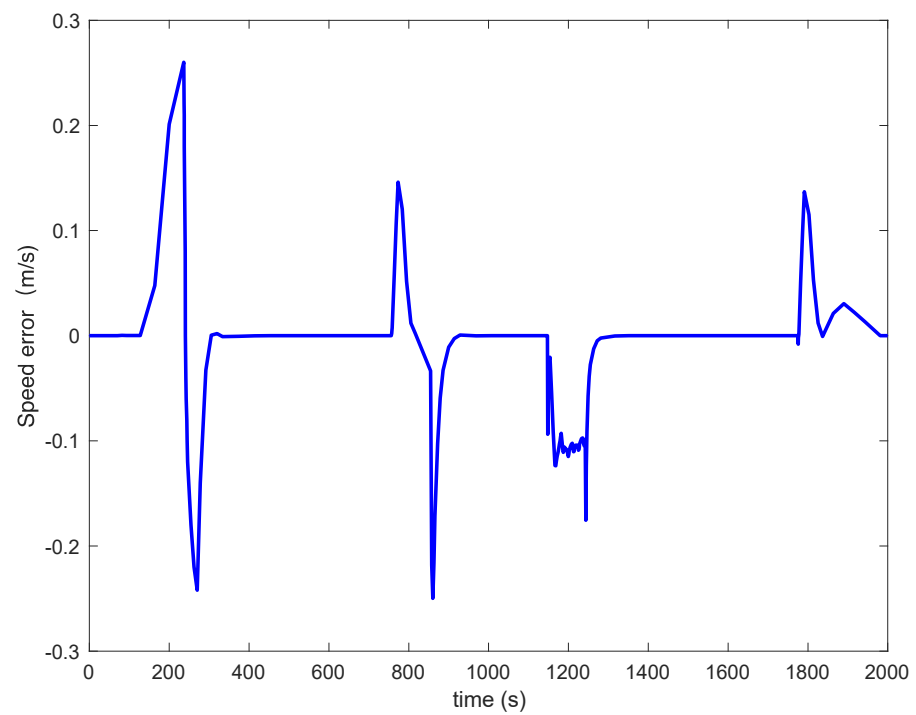
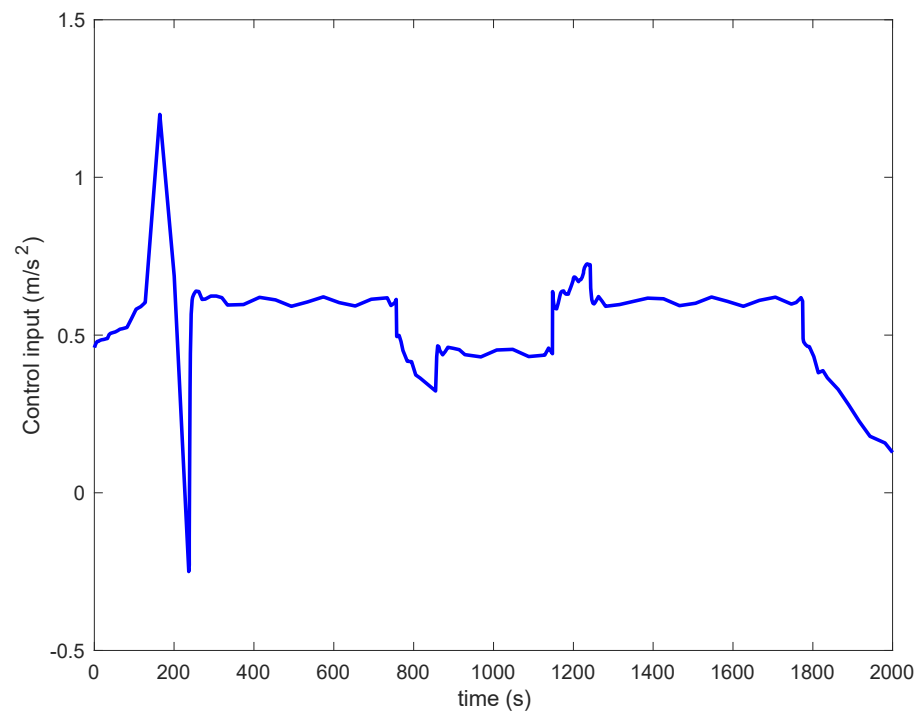


Figure 7. Speed error.



**Figure 8.** Control input.

It can be seen from Figure 4 that the position tracking curve was closely attached and there was no system overshoot phenomenon, indicating that the tracking effect of the controller was good. At the same time, it can be seen from Figure 5 that, under the system model parameters and complex route conditions of the train operation, the results could converge quickly, and the position signal was bounded, thus identifying the given train position curve with high precision. When the train operated on a route with a large slope and complex curve, the control accuracy of RBFNN-POCRAC controller decreased due to the strong additional resistance and external interference, but the position tracking error was still less than 0.2 m, thus meeting the requirements of train parking accuracy. Therefore, the RBFNN-POCRAC controller not only ensures the stable operation of the train on the route with a large slope and complex curve, but also achieves a final parking accuracy of almost 0, thereby meeting the control requirements.

According to the speed tracking performance in Figure 6 and the speed tracking error in Figure 7, when the initial speed was 0, the controller could track the given train speed curve with small error, and the speed signals were bounded. When the train was operating on a complex route with a large slope and smaller curve radius, the speed tracking fluctuated due to the strong disturbance from the outside, and the speed error was  $-0.24$  m/s to  $0.26$  m/s, but the speed tracking error of the remaining routes was almost zero. Therefore, the RBFNN-POCRAC algorithm proposed in this paper can ensure the safety of train operation.

Figure 8 shows the train control input curve of the RBFNN-POCRAC algorithm, i.e., the acceleration curve of train operation. When the train started, it needed to overcome its own gravity and other unknown disturbances, and the maximum acceleration value was  $0.48$  m/s<sup>2</sup>. When the train was operating from 52 s to 248 s, in order to overcome the interference of the slope and curve, the controller quickly switched the control input to maintain the control accuracy. When the train was operating in the common route section, the change in acceleration of the control train operation was small, and it was basically kept at about  $0.6$  m/s<sup>2</sup>, which improved the comfort of the train operation to a certain extent. At the same time, for the whole train's fully automatic operation, the switching times of traction and braking were less, which effectively improved the service life and effective period of the traction or braking mechanism.

## 6.2. Controller Performance Comparison

As we all know, the PID control algorithm is widely used in train operation control, such as the Beijing Metro Yizhuang Line. In order to prove the advantages of the RBFNN-POCRAC controller in terms of control accuracy and anti-interference, this paper chose position output-constrained robust adaptive control (POCRAC), PID control, and RBFNN-PID control in the literature [30] as the comparison objects, loaded the same desired tracking curve shown in Figure 3, and compared the tracking error of the four controllers.

It can be seen from Figure 9 that the RBFNN-POCRAC controller converged quickly to the whole process of desired position tracking in the face of strong additional resistance and external interference. When the train ran to 158 s, the position error reached the maximum value of 0.142 m, and the position tracking error at other times was almost zero, showing strong anti-interference ability. When the POCRAC controller faced external interference, the position error convergence was slow, and the maximum position error was 0.2 m. PID control and RBFNN-PID control exhibited a large position error throughout the process of train operation, being far greater than the 0.2 m position error defined in this article. The position error of PID control fluctuated greatly, and the control performance was poor. Compared with PID, RBFNN-PID control effectively reduced the position error of train operation control; however, under the condition of uncertain model parameters and external interference, the position error was significantly larger than the controller designed in this paper.

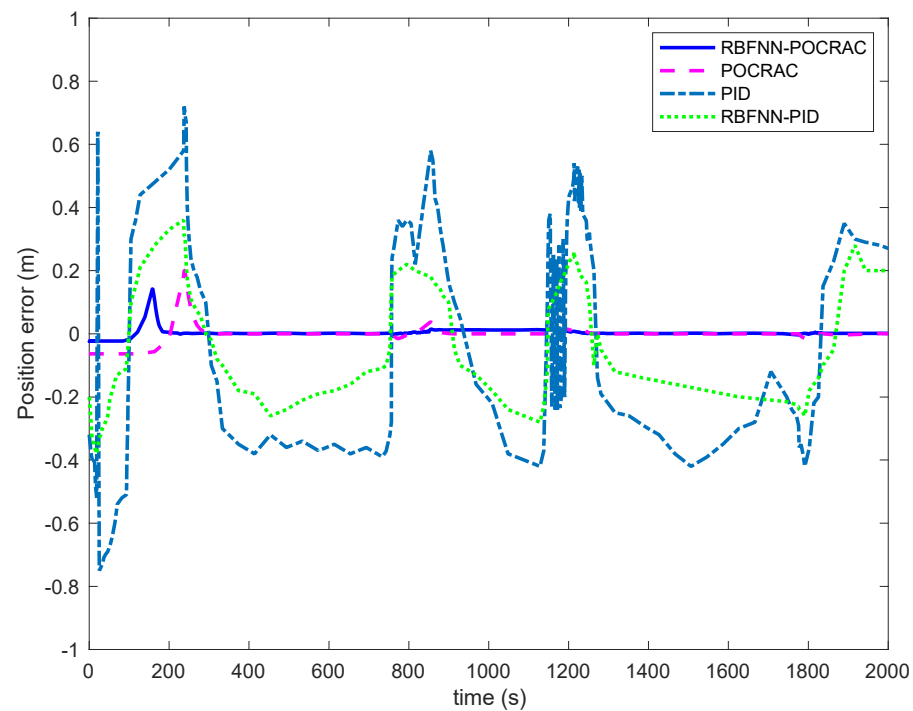
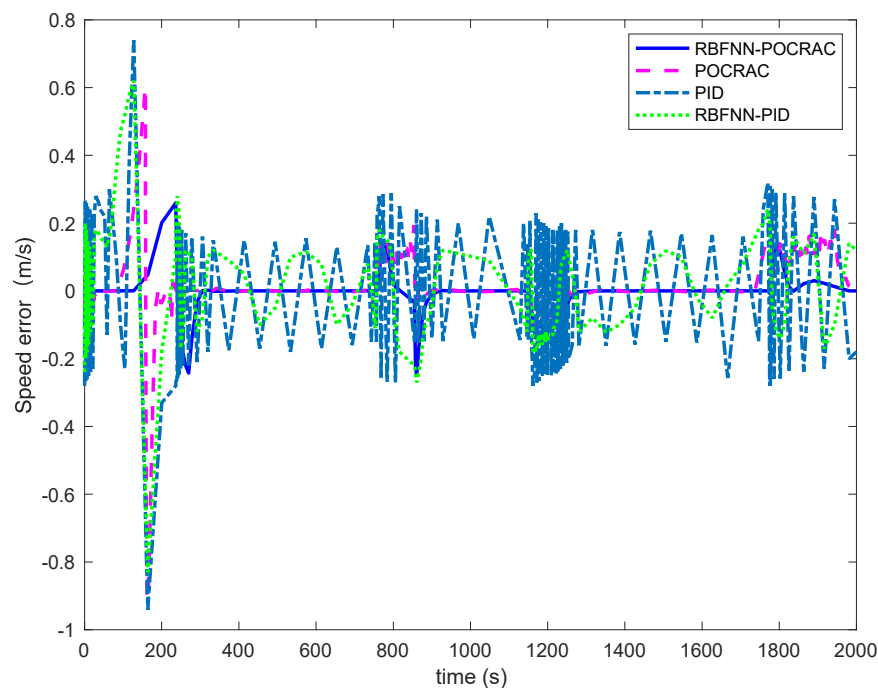


Figure 9. Position error comparison.

It can be seen from Figure 10 that when the four controllers faced strong additional resistance and external interference, the train running speed error of the RBFNN-POCRAC controller was the smallest, and the train running speed error and fluctuation of the PID controller were the largest. Compared with the PID control method, RBFNN-PID control obviously alleviated the speed error, but it was still greater than the speed tracking error of the POCRAC controller and RBFNN-POCRAC controller. The POCRAC controller lacked the ability to adapt to the strong additional resistance and external interference, leading to a certain overshoot of the operation speed, and the control performance was not ideal.



**Figure 10.** Speed error comparison.

It can be seen from Figures 9 and 10 that the RBFNN-POCRAC controller had the fastest convergence speed and the smallest overall position error and speed error in the face of the uncertain model parameters, strong additional resistance, and external interference, and it had good control performance and strong adaptive ability, which could ensure the safe and reliable operation of the train, has along with universal engineering practicability.

In order to further illustrate the control effect of the RBFNN-POCRAC controller, this paper changed the train model parameters of the four controllers within the range of  $\pm 10\%$  and performed 100 simulation runs. The comparison results of the position error range, speed error range, and average parking accuracy are shown in Table 2. It can be seen that the RBFNN-POCRAC controller had the best position and speed tracking performance and the highest parking accuracy, and it could adapt to the external environment of train operation and the changes in train dynamics model parameters, thus meeting the requirements of FAO's high-precision operation control.

**Table 2.** Performance comparison of control methods.

Control Method	Position Error (m)	Speed Error (m/s)	Average Stopping Accuracy (m)
RBFNN-POCRAC	[−0.084, 0.178]	[−0.28, 0.32]	0.0016
POCRAC	[−0.162, 0.2]	[−0.95, 0.77]	0.048
RBFNN-PID	[−0.46, 0.52]	[−0.98, 0.84]	0.229
PID	[−1, 1.5]	[−1.04, 0.92]	0.387

Table data obtained by 100 simulation runs.

## 7. Discussion

FAO is a new-generation rail transit control system that realizes automation of the whole process of train operation. It is the development direction of the automatic train operation system (ATO) toward artificial intelligence. FAO is based on an unmanned driving function, combined with on-board information and route information, according to the desired speed and position curve, thus automatically controlling the operating process of the train and realizing functions such as the automatic adjustment of train speed, operating time, and precise parking so as to ensure the train's operation in the best state. In recent years, urban rail transit systems around the world have been applied, such as

Beijing Yanfang Line. The control method applied in FAO is still commonly represented by PID control in ATO, as well as the combination of PID and other control algorithms. Although it can meet the requirements of the train safe operation, the control input of the PID controller fluctuates frequently and the control accuracy is not high, especially in regions with complicated slopes and curves, which affects the control performance of train operation and the comfort of passengers.

The key to the design of an FAO controller is to establish an accurate train dynamics model. However, the dynamic process of train operation is related to multiple factors, and it is impossible to establish an accurate train dynamics model. In addition, different train types, routes, passenger capacity, weather, and temperature will cause changes in model parameters. Therefore, the train dynamics model in FAO mostly adopts a single particle, as the factors considered in multiparticle train dynamics models are too complicated, which is not conducive to the design of an FAO controller and the automatic control of train operation.

In summary, in future FAO design, single-particle dynamics models should be selected as much as possible, and an adaptive mechanism should be introduced to deal with the uncertainty of model parameters and the variability of the external environment of train operation. At the same time, control algorithms that can improve the response speed, control accuracy, and passenger comfort should be selected to improve the FAO's control performance and provide strong technical support for urban rail transit to become more intelligent.

## 8. Conclusions

Because different train types, routes, and even different weather conditions affect the establishment of a train dynamic model, and because the relationship between train resistance and speed is highly nonlinear, it is not feasible to accurately obtain a dynamic model of train motion. Thus, RBFNN was used to approximate the additional resistance and unknown disturbance dynamics of train operation, and the adaptive mechanism of the Davis equation coefficient of basic resistance was introduced to enhance the robustness and adaptability of the control system. At the same time, aiming at precise control technology in the FAO, the RBFNN-POCRAC algorithm was proposed, and a simulation platform was used to verify the proposed control algorithm. When the FAO had parameter uncertainty, time-varying parameters, strong additional resistance, and external disturbance, the proposed control algorithm could achieve smooth, fast, and accurate tracking for the desired curve.

Combined with the research content of this paper, future research work will mainly include two aspects:

- Research on FAO control methods based on deep learning and knowledge automation. The existing control methods do not fully utilize the massive data generated by the train operation. However, the deep learning method can generate “strategic” data for the train operation control system. Combining deep learning and knowledge automation control methods, mining rules from the “strategic” data, and making accurate predictions will help real-time monitoring and automatic adjustment of the train operation status.
- Research on coordinated control methods for multi-train tracking operation. The purpose of multi-train coordinated control is to increase the traffic density by adjusting the minimum safe interval between the preceding train and the following train. FAO combined with multi-train cooperative control can effectively reduce the overall energy consumption and life-cycle cost of the system, which is the future development direction of urban rail transit.

**Author Contributions:** Conceptualization, J.Y. and Y.Z.; methodology, J.Y. and Y.Z.; software, J.Y. and Y.Z.; validation, J.Y., Y.Z. and Y.J.; formal analysis, J.Y. and Y.J.; investigation, J.Y. and Y.J.; resources, J.Y.; data curation, J.Y. and Y.J.; writing—original draft preparation, J.Y.; writing—review

and editing, J.Y.; visualization, J.Y., Y.Z. and Y.J.; supervision, Y.Z. All authors have read and agreed to the published version of the manuscript.

**Funding:** This research was funded by NSFC, grant number 61963023.

**Institutional Review Board Statement:** Not applicable.

**Informed Consent Statement:** Not applicable.

**Data Availability Statement:** The data are contained within the article.

**Conflicts of Interest:** The authors declare no conflict of interest. The funders had no role in the design of the study; in the collection, analyses, or interpretation of data; in the writing of the manuscript, or in the decision to publish the results.

## References

1. Gao, C.H. Rail train operation control system based on communication. *Mod. Urban Transit.* **2007**, *2*, 7–10.
2. Gao, C.H. Study on ATO braking model identification based on model selection and optimization techniques. *J. China Railw. Soc.* **2011**, *33*, 56–60.
3. Yin, J.; Tang, T.; Yang, L. Research and development of automatic train operation for railway transportation systems: A survey. *Transp. Res. Part C Emerg. Technol.* **2017**, *85*, 548–572. [[CrossRef](#)]
4. Dong, H.R.; Gao, S.G.; Ning, B. Extended fuzzy logic controllers for high speed train. *Neural Comput. Appl.* **2013**, *22*, 321–328. [[CrossRef](#)]
5. Tan, L.T.; Huang, Y.N.; Li, L.Y. Driving curve algorithm for heavy haul train based on improved BP Neural Network. *Railw. Comput. Appl.* **2016**, *25*, 1–5.
6. Shi, W.S. Research on automatic train operation based on model-free adaptive control. *J. China Railw. Soc.* **2016**, *38*, 72–77.
7. Wu, P.; Wang, Q.Y.; Feng, X.Y. Automatic train operation based on adaptive terminal sliding mode control. *Int. J. Autom. Comput.* **2015**, *12*, 142–148. [[CrossRef](#)]
8. Yin, J.; Chen, D.; Li, Y. Smart train operation algorithms based on expert knowledge and ensemble CART for the electric locomotive. *Knowl.-Based Syst.* **2016**, *92*, 78–91. [[CrossRef](#)]
9. Wang, P.L.; Wang, Q.Y.; Cui, H.B. Automatic train operation algorithm for train tracking. *J. Southwest Jiaotong Univ.* **2013**, *48*, 1045–1051.
10. He, Z.Y.; Xu, N. Automatic train operation algorithm based on adaptive iterative learning control theory. *J. Transp. Syst. Eng. Inf. Technol.* **2020**, *20*, 69–75.
11. Cao, Y.; Zhang, Y.Z. Application of fuzzy predictive control technology in automatic train operation. *Clust. Comput.* **2018**, *22*, 78–85. [[CrossRef](#)]
12. Li, Z.X.; Hou, Z.S. Adaptive iterative learning control based high-speed train operation tracking under iteration varying parameter and measurement noise. *Asian J. Control* **2015**, *17*, 1–10. [[CrossRef](#)]
13. Yang, Y.F.; Cui, K.; Lv, X.J. Combined sliding model and PID control of automatic train operation system. *J. China Railw. Soc.* **2014**, *36*, 61–67.
14. Wang, Q.Y.; Wu, P. Precise automatic train stop control of algorithm based on adaptive terminal sliding mode control. *J. China Railw. Soc.* **2016**, *38*, 56–63.
15. Lian, W.B.; Liu, B.H. Automatic operation speed control of high-speed train based on ADRC. *J. China Railw. Soc.* **2020**, *42*, 76–81.
16. Gao, S.G. On several control problems of multi-train cooperation. *Beijing Jiaotong Univ.* **2016**, *6*, 7–10.
17. Davis, W.J. The tractive resistance of electric locomotives and cars. *Gen. Electr.* **1926**, *2*, 26–32.
18. Hartman, E.J.; Keeler, J.D.; Kowalski, J.M. Layered neural networks with Gaussian hidden units as universal approximations. *Neural Comput.* **1990**, *2*, 210–215. [[CrossRef](#)]
19. Park, J.; Sandberg, L.W. Universal approximation using radial-basis-function networks. *Neural Comput.* **1991**, *3*, 246–257. [[CrossRef](#)]
20. Broomhead, D.S.; Lowe, D. Radial basis functions multi-variable functional interpolation and adaptive networks. *Tech. Rep.* **1988**, *26*, 32–39.
21. Wang, S.W.; Yu, D.L. Adaptive RBF network for parameter estimation an stable air-fuel ratio control. *Neural Netw.* **2008**, *21*, 102–112. [[CrossRef](#)]
22. Zhu, Q.; Fei, S.; Zhang, T.; Li, T. Adaptive RBF neural-networks control for a class of time-delay nonlinear systems. *Neurocomputing* **2008**, *71*, 3617–3624. [[CrossRef](#)]
23. Qu, Y.Y.; Zuo, L.; Zhang, E.D. Algorithm for structure design of RBF neural network based on parameter optimization. *J. Northeast. Univ.* **2020**, *41*, 176–182.
24. Fan, J.H.; Jia, S.M.; Li, X.Z. Adaptive control for omni-directional intelligent wheelchairs based on RBF neural network. *J. Huazhong Sci. Technol. Univ.* **2014**, *42*, 111–115.
25. Zeng, Z.Z. Feedback compensation control on chaotic system with uncertainty based on radial basis function neural network. *Chin. Phys. Soc.* **2013**, *62*, 1–6.
26. Fu, D.X.; Zhao, X.M. Backstepping terminal sliding mode control based on radial basis function neural network for permanent magnet linear synchronous motor. *Trans. China Electrotech. Soc.* **2020**, *35*, 2546–2554.

27. Li, Z.; Hou, Z.; Yin, C. Iterative learning control for train trajectory tracking under speed constrains with iteration-varying parameter. *Trans. Inst. Meas. Control* **2015**, *37*, 485–493. [[CrossRef](#)]
28. Ren, B.B.; Ge, S.S.; Tee, K.P. Adaptive neural control for output feedback nonlinear systems using a barrier Lyapunov function. *IEEE Trans. Neural Netw.* **2010**, *21*, 1339–1345.
29. Tee, K.P.; Ge, S.S.; Tay, E.H. Barrier Lyapunov functions for the control of output-constrained nonlinear systems. *Automatic* **2009**, *45*, 918–927. [[CrossRef](#)]
30. Xiao, L.; Liang, X.R.; Wang, X.Q. RBF neural network PID control for tracking speeds of high-speed trains. *J. Wuyi Univ.* **2020**, *34*, 24–31.